Research Square

Preprints are preliminary reports that have not undergone peer review.
They should not be considered conclusive, used to inform clinical practice,
or referenced by the media as validated information.

Zika Virus Infection Triggers Interferon-Dependent Downregulation of Prolyl Oligopeptidase Activity in the Neonatal Brain

Ana P. Ximenes
Universidade Federal de São Paulo
Ingrid S. de Farias
Universidade Federal de São Paulo
William Y. Oyadomari
Universidade Federal de São Paulo
Leonardo Basso
Universidade Federal de São Paulo
Raissa Rilo Christoff
Universidade Federal do Rio de Janeiro
Tailene Rabello
Universidade Federal do Rio de Janeiro
Luiza M. Higa
Universidade Federal do Rio de Janeiro
Patrícia P. Garcez
Universidade Federal do Rio de Janeiro
Mirian A. F. Hayashi
mhayashi@unifesp.br

Universidade Federal de São Paulo

Article

Keywords: flavivirus, neuroinflammation, neurodevelopment, interferon signaling, innate immune activation, neurotrophic responses

Posted Date: April 21st, 2026

DOI: https://doi.org/10.21203/rs.3.rs-9216258/v1

License: This work is licensed under a Creative Commons Attribution 4.0 International License.
Read Full License

Additional Declarations: No competing interests reported.

Abstract

Flaviviruses pose a persistent threat to global health; notably, Zika virus (ZIKV) became a focal point of international research during the 2015–2016 Brazilian epidemic due to its association with congenital microcephaly. Although distinct viral lineages are associated with varying pathogenic outcomes, the precise molecular mechanisms driving neuroimmune responses in the developing brain remain poorly defined. Here, we investigated whether neonatal ZIKV infection modulates the activity of the serine protease prolyl oligopeptidase (POP), an enzyme implicated in neuroinflammatory and neuroplasticity regulation. The interplay between POP activity and immune response was also investigated comparing two distinct ZIKV lineages. Newborn mice were infected at postnatal day 0 with either the Brazilian ($ZIKV^{BR}$) or African ($ZIKV^{AF}$) strain. We then assessed POP activity, neuroinflammatory markers, interferon signaling and neurotrophic responses at postnatal days 3 (P3) and 7 (P7). At P3, both strains triggered robust innate immune activation - with $ZIKV^{AF}$ eliciting a stronger pro-inflammatory while POP activity remained unaltered. By P7, however, $ZIKV^{BR}$ infection drove a sustained inflammatory and interferon signaling response that was accompanied by a significant reduction in POP activity. Administration of exogenous IFN-β, at a dosage and regimen previously shown to prevent microcephaly, recapitulated the virus-induced reduction in POP activity. This indicates that type I interferon signaling directly drives this modulation. Together, these findings reveal a novel neuroimmune axis where prolonged, ZIKV-induced Type I interferon signaling suppresses POP activity, highlighting a mechanism by which sustained antiviral responses may alter neurodevelopmental trajectories.

1. Introduction

Flavivirus infections remain a major global health concern due to their capacity to cause widespread outbreaks and severe clinical manifestations. Among them, Zika virus (ZIKV) has gained prominence for its strong tropism for developing brain and association with a congenital syndrome characterized by microcephaly and other neurodevelopmental impairments[1–3]. The large ZIKV epidemic in Brazil in 2016 underscored this threat by establishing a clear link between maternal infection during pregnancy and foetal brain malformations, which prompted the World Health Organization (WHO) to declare a public health emergency[4,5].

Importantly, it is well known that ZIKV viral strains differ in virulence[6]. The African lineage ($ZIKV^{AF}$, MR-766) displays higher cytopathogenicity, infecting neurons, astrocytes, and neural progenitor cells, often inducing cell death and hippocampal degeneration, associated with miscarriage and severe foetal cases[7]. Conversely, this virus strain has been associated with mild symptoms, such as fever, rash, and conjunctivitis, with no reported cases of microcephaly or significant outbreaks. In contrast, the Brazilian strain ($ZIKV^{BR}$) has been detected in placental tissue, amniotic fluid, and brains of microcephalic foetuses with strong association with congenital malformations despite less virulent and less intense induction of pro-inflammatory cytokines[8]. These differences highlight the complex relationship between viral genetics, host immune responses, and neuropathology.

Innate immune responses play a central role in ZIKV pathogenesis. During the early stages of infection, host innate immunity rapidly activates pro-inflammatory cytokines, including IL-6, TNF-α, and IL-1β, and triggers the type I interferon (IFN-I) signaling pathway through pattern recognition receptors (PRRs), mainly RIG-I–like receptors (RLRs) and Toll-like receptors (TLRs)[9,10]. IFN-I subsequently induces the expression of hundreds of interferon-stimulated genes (ISGs), which interfere with multiple steps of the viral life cycle, including viral entry, genome replication, protein translation, and virion release[11,12]. Through these mechanisms, IFN-I signaling plays a critical role in controlling viremia and limiting systemic viral spread. The importance of this pathway is highlighted by studies showing that mice lacking the interferon-α/β receptor (IFNAR) exhibit markedly elevated viral loads in the brain and spinal cord, develop severe neurological symptoms, and ultimately succumb to infection[10]. However, ZIKV has evolved several strategies to antagonize IFN-I signaling and thereby modulate disease outcomes[13]. A productive infection is established by ZIKV by dictating sophisticated strategies to antagonize the IFN-I network. ZIKV severely dampens downstream IFNAR signaling while simultaneously inhibiting upstream IFN-I induction[14], revealing virus-specific responses leading to microcephaly[15]. These mechanisms suggest that ZIKV can manipulate antiviral signaling pathways and adapt to tissue-specific immune environments by modulating the ISG antiviral network.

In addition, beyond canonical innate immune system pathways, other modulators may also contribute to neuroimmune balance. For instance, the serine protease prolyl oligopeptidase (POP, also known as PREP), has been implicated in neuropeptide processing, inflammation, and neurodegeneration[16], and more recently has emerged as a potential biomarker and therapeutic target in neurodegenerative diseases characterized by neuroinflammatory processes[17,18].

This multifunctional serine protease with growing biomedical interest was first described over 50 years ago as an oxytocin-cleaving enzyme[19]. POP is widely expressed in mammalian tissues, particularly in the brain, where it regulates neuropeptide processing, synaptic plasticity, and inflammatory responses, leading to be recognized as a neurospecific biomarker of neuroinflammation with potential relevance for neuroprotective strategies[17]. POP also participates in the renin-angiotensin system (RAS) through angiotensin II metabolism[20], while also processing thymosin-β4 into the anti-inflammatory tetrapeptide Ac-SDKP[21]. Altered POP activity has been described in multiple sclerosis, cirrhosis, depression (POP was decreased in patients treated with lithium), and neurodegeneration, while its inhibition shows neuroprotective and anti-inflammatory effects in various disease models[16,22,23]. Although altered POP activity has been reported in multiple conditions involving CNS inflammation, its role during viral infections remains unexplored. Emerging research suggests POP's involvement in immune responses, potentially by regulating peptide hormones or inflammatory mediators. For instance, some studies link POP inhibition to anti-inflammatory effects or modulation of cytokine production[24]. Thus, evidence that POP may perform a central part in inflammation paves the road to further investigation into such molecular targets, which hold significant promise for advancing both diagnostic capabilities and the development of effective antiviral strategies against these globally significant pathogens.

Thus, we investigated whether ZIKV infection modulates POP activity in the neonatal brain and whether these changes are associated with antiviral immune responses, particularly IFN-I signaling. Using a neonatal mouse model, we show that ZIKV infection induces robust inflammatory and ISGs responses. Notably, POP activity remained unchanged at early stages of infection (postnatal day 3 - P3), although significantly reduced at a later developmental stage (postnatal day 7 - P7) following $ZIKV^{BR}$ infection via either intraperitoneal (IP) or intracerebroventricular (ICV) routes. Moreover, treatment with exogenous IFN-β - previously shown to prevent microcephaly in this model - was sufficient to reproduce the reduction in POP activity even in the absence of viral infection. This reduction coincided with the upregulation of ISGs such as *Oas1g* and *Ifit1*, indicating that antiviral immune signaling may influence POP activity during ZIKV infection in the developing brain.

2. Results

2.1 Differential modulation of innate immune gene expression by Brazilian and African ZIKV strains

Newborn Swiss mice (P0) were infected by intracerebroventricular (ICV) route with either the Brazilian ($ZIKV^{BR}$) or the African ZIKV strain ($ZIKV^{AF}$). Control animals (mock) received uninfected C6/36 conditioned medium (vehicle). Molecular analyses were restricted to postnatal day 3 (P3) due to the high lethality associated with $ZIKV^{AF}$ infection observed in our experiments, also as previously reported by others[6].

The early neuroinflammatory response was characterized by quantifying the mRNA levels of canonical pro-inflammatory cytokines such as *Il6*, *Tnf*, and *Il1b* (Fig. 1A-C), ISGs (including *Oas1g* and *Ifit1*) (Fig. 1D, E), and components of the IFNAR complex (*Ifnar1* and *Ifnar2*) (Fig. 1F, G). Both ZIKV strains robustly increased the expression of both pro-inflammatory cytokines (Fig. 1A-C), *Oas1g* and *Ifit1* (Fig. 1D, E), indicating a rapid activation of innate immune pathways in the neonatal brain following infection. In contrast, no significant differences were detected in the expression of *Ifnar1* (Fig. 1F) or *Ifnar2* (Fig. 1G) compared to their respective mock control groups. These findings suggest that, despite the strong induction of interferon-stimulated genes, transcriptional modulation of IFNAR components is not a prominent feature of the early response at this infection stage.

Sustained inflammatory and antiviral signaling can influence neuronal homeostasis and plasticity in the developing brain[25,26]. Genes associated with neurotrophic support were also examined here. Among these neurotrophins, Brain-Derived Neurotrophic Factor (BDNF) plays a central role in neuronal survival and synaptic plasticity and bridges the gap between environmental stimuli, neuronal survival, and cognitive resilience by promoting changes in synaptic connections and supporting the survival of newly generated neurons (neurogenesis)[27,28]. Analysis of mRNA levels revealed a significant reduction in *Bdnf* expression in $ZIKV^{BR}$-infected animals compared with mock controls (Fig. 1H). Conversely, *Bdnf* expression was not significantly changed by $ZIKV^{AF}$ infection. These results indicate that infection with

the Brazilian strain, but not the African strain, is associated with reduced *Bdnf* expression in the neonatal brain at this early time point of infection.

Direct comparison between these two viral strains revealed a markedly relative stronger inflammatory response in ZIKV^{AF}-infected mice. In fact, expression levels of *Il6*, *Tnf*, *Il1b*, *Oas1g*, *Ifit1*, *Ifnar1*, and *Bdnf* (Fig. 1A-F) were consistently higher in ZIKV^{AF} relative to ZIKV^{BR} animals, whereas *Ifnar2* expression was not modulated by the ZIKV infection (Fig. 1G). This increased transcriptional response induced by ZIKV^{AF} aligns with its pronounced cytopathogenicity, which manifests as increased neuronal death and hippocampal degeneration in severe fetal cases[6,7]. Although ZIKV^{BR} was strongly associated with congenital ZIKV syndrome and microcephaly[15,29], our present data indicate that, at P3, ZIKV^{AF} triggers a more pronounced early innate immune activation in the neonatal brain.

Despite this robust inflammatory and interferon-related transcriptional response, POP activity remained unchanged at P3 in ZIKV^{BR}- and ZIKV^{AF}-infected mice (Fig. 1I). This finding suggests that, during this early developmental window - when mice undergo the final major waves of neurogenesis, roughly corresponding to the mid-third trimester of human gestation (30–34 weeks) - POP activity is not directly modulated regardless of the acute ZIKV-induced inflammation.

POP-null mice exhibit altered growth cone dynamics and deficits in synaptic plasticity[30,31]. Because postnatal day 7 (P7) represents a critical developmental period characterized by intense synaptogenesis, dendritic arborization, the onset of myelination, and active gliogenesis, we hypothesized that POP activity regulation might emerge at later stages of infection, potentially in response to sustained neuroinflammation or prolonged antiviral signaling.

2.2 Sustained inflammatory and interferon responses in ZIKV^{BR}-infected neonatal brain at postnatal day 7

The impact of prolonged infection on innate immune signaling was assessed through subsequent analyses including only ZIKV^{BR}-infected animals which were able to survive beyond 7 days post-infection (dpi).

At P7, ZIKV^{BR}-infected neonatal brains displayed a robust inflammatory profile compared with mock controls. Significant upregulation of *Il6* (Fig. 2A), *Tnf* (Fig. 2B), *Il1b* (Fig. 2C), *Oas1g* (Fig. 2D), and *Ifit1* (Fig. 2E) was noticed. In contrast to the early infection time point (at P3), expression of *Ifnar1* (Fig. 2F) was significantly reduced, whereas *Ifnar2* (Fig. 2G) levels remained unchanged, suggesting a dynamic modulation of the IFNAR complex during ongoing infection.

Analysis of neurotrophic signaling at P7 revealed that *Bdnf* expression was significantly increased in ZIKV^{BR}-infected animals compared with mock controls (Fig. 2H), indicating that neurotrophic pathways become engaged as infection progresses.

Direct temporal comparison between P3 and P7 for ZIKV^{BR}-infected mice revealed selective changes in the inflammatory response in neonatal brains. Among pro-inflammatory cytokines, *Il6* expression increased from 2.5-fold at P3 to 9.8-fold at P7 ($p = 0.0289$), indicating a significant amplification along infection progress. In contrast, *Tnf* and *Il1b* expression did not differ significantly between P3 and P7 (Table 1). Conversely, significant temporal amplification of classical ISGs expression was observed. While *Oas1g* increased from 142.9-fold at P3 to 272.1-fold at P7 ($p = 0.0033$), *Ifit1* increased from 144.0-fold to 326.0-fold ($p = 0.0420$), indicating a sustained and intensified antiviral signaling during infection progression. In contrast, expression of the interferon receptor subunits *Ifnar1* and *Ifnar2* did not differ significantly between P3 and P7 (Table 1). This divergence between receptor expression and robust ISG induction suggests sustained antiviral signaling, highlighting that even later into the infection, there is a persistent, active antiviral and inflammatory state in the tissue[32,33]. This sustained downstream signaling, which occurs without receptor upregulation, strongly supports our hypothesis that prolonged neuroinflammation alters neurodevelopment[34,35].

Consistent with these temporal changes in immune signaling, *Bdnf* expression differed significantly between P3 and P7. Expression increased from 0.7-fold at P3 to 1.8-fold at P7 ($p = 0.0091$), indicating a significant temporal increase along infection progression.

Together, these findings indicate that ZIKV^{BR} infection sustains and dynamically reorganizes neuroinflammatory and antiviral signaling throughout early postnatal development. This evolving balance between inflammatory mediators, interferon signaling, and neurotrophic responses suggests that the infected neonatal brain attempts to adapt to persistent viral stress while maintaining antiviral defense mechanisms.

Table 1

Temporal changes in gene expression between P3 and P7 in ZIKV-infected neonatal brains. Fold change values represent relative expression compared with time-matched mock controls ($2^{-\Delta\Delta Ct}$). Temporal change (P7/P3) represents the ratio between fold changes at P7 and P3. Statistical comparisons between P3 and P7 were performed using Welch-corrected t-tests.

Functional category	Gene	Fold change P3	Fold change P7	P7/P3	*p*-value
Pro-inflammatory cytokines	*Il6*	2.5	9.8	3.9	0.0289
	Tnf	3.0	3.5	1.1	0.7286
	Il1b	9.2	13.1	1.4	0.2982
Interferon-stimulated genes (ISGs)	*Oas1g*	142.9	272.1	1.9	0.0033
	Ifit1	144.0	326.0	2.2	0.0420
Type I interferon receptors	*Ifnar1*	0.7	0.5	0.7	0.1248
	Ifnar2	1.8	1.2	0.7	0.3926
Neurotrophic signaling	*Bdnf*	0.7	1.8	2.6	0.0091

2.3 Delayed downregulation of POP activity in ZIKV^{BR} infection

Given the sustained and evolving inflammatory landscape at P7, we next investigated whether prolonged infection modulates POP activity in the neonatal brain.

At P7, POP activity was significantly reduced in brains from neonatal mice infected via the intracerebroventricular (ICV) route (4.8 ± 1.0 μM/min) compared with mock-infected controls (5.8 ± 1.3 μM/min; F = 9.300, *p* = 0.0006) (Fig. 3). Notably, a similar decrease was also observed in animals infected via intraperitoneal (IP) administration (mock: 6.9 ± 1.1 μM/min; ZIKV^{BR}: 5.2 ± 1.4 μM/min; F = 4.578, *p* = 0.0154) (Supplemental Fig. 1), indicating that POP downregulation represents a consistent feature of ZIKV infection irrespective of the infection route or vertical transmission.

Importantly, POP activity remained unchanged at the early infection time point (P3) (Fig. 1I) regardless of early innate immune activation. In addition, the reduction in POP activity triggered by ZIKV infection appears to emerge only at later stages of infection.

Together, these findings demonstrate that ZIKV infection induces a delayed downregulation of POP activity in the neonatal brain, independent of the initial inflammatory response and despite the suggested role of POP in driving inflammation[36,37]. These findings suggest that POP upregulation is driven by sustained inflammatory signaling, ongoing viral replication, or secondary changes in the neural microenvironment rather than the immediate innate immune response.

2.4 Type I interferon (IFN-I) signaling induces POP downregulation during ZIKV^{BR} infection

IFN-I represent a central component of antiviral innate immunity, acting primarily by restricting viral replication and ISGs induction. Given the strong activation of the IFN pathway observed at P7 together with the concomitant reduction in POP activity, we next investigated whether IFN-I signaling could account for the observed decrease in POP activity during ZIKV^{BR} infection.

Neonatal mice were treated with exogenous IFN-β under the same experimental conditions previously shown to mitigate ZIKV^{BR}-induced microcephaly[25]. At P7, both ZIKV^{BR} infection and IFN-β treatment independently resulted in significant reductions in POP activity compared with mock controls (mock: 5.0 ± 1.5 μM/min; ZIKV^{BR}: 1.8 ± 1.3 μM/min; mock + IFNβ: 1.7 ± 0.9 μM/min; F = 8.667, *p* = 0.0008) (Fig. 4). Importantly, POP activity did not differ significantly between ZIKV^{BR}-infected animals and uninfected animals treated with IFN-β, nor between ZIKV^{BR} and ZIKV^{BR} + IFNβ groups. These results indicate that IFN-I signaling alone is sufficient to recapitulate the viral-induced reduction in POP activity, an effect that is not further suppressed by exogenous IFN-β administration. Furthermore, IFN-β treatment neither rescued nor further exacerbated the decrease in POP activity induced by ZIKV^{BR} infection (Fig. 4). This lack of an additive effect suggests that activation of the IFN pathway is a primary upstream driver of

POP modulation, a finding consistent with previous reports of reduced POP activity following IFN-α immunotherapy[38].

Together, these findings demonstrate that IFN-I signaling induces POP downregulation in the neonatal brain, indicating that immune-mediated mechanisms, rather than direct viral cytopathological effects alone, likely contribute to the modulation of POP activity during ZIKV infection.

3. Discussion

In the present study, we show that neonatal ZIKV infection induces a temporally dynamic neuroimmune response in the developing brain, characterized by an early inflammatory activation that precedes a significant downregulation of POP activity. Both $ZIKV^{BR}$ and $ZIKV^{AF}$ infection triggered robust induction of pro-inflammatory cytokines and ISGs at P3, indicating rapid activation of innate immune pathways. However, despite this pronounced early inflammatory response, POP activity remained unchanged at this early infection stage. Notably, a significant reduction in POP activity, accompanied by sustained interferon-driven antiviral signaling, was observed only at P7. Importantly, administration of exogenous IFN-β recapitulated the virus-induced reduction in POP activity, indicating that activation of IFN-I signaling is key and sufficient to modulate POP activity in the neonatal brain.

Consistent with previous reports describing differential virulence among ZIKV lineages[6], $ZIKV^{AF}$ induced a stronger pro-inflammatory response at P3 compared with $ZIKV^{BR}$. Increased expression of *Il6, Tnf, Il1b, Oas1g*, and *Ifit1* indicates a rapid activation of innate immune pathways in the neonatal brain, a response commonly associated with flavivirus infections[39,40]. Despite pronounced early inflammatory activation, transcript levels of the IFN-I receptors *Ifnar1* and *Ifnar2*, as well as POP activity, remained comparable to mock controls. Notably, even the markedly stronger inflammatory response induced by the $ZIKV^{AF}$ strain failed to alter POP activity during this early phase, indicating that this acute cytokine-driven inflammation alone is insufficient for POP modulation.

This observation is particularly relevant considering that P3 corresponds to a developmental stage when mice undergo the final major waves of neurogenesis, roughly equivalent to the mid-third trimester of human gestation (30–34 weeks)[41]. During this period, neuronal progenitors, differentiating neurons, and glial cells coexist within a highly dynamic microenvironment. These features suggest that POP activity was not affected by ZIKV infection during early neurodevelopment, despite the exacerbated inflammatory signals in response to viral infection at early stage.

In addition, we demonstrate the inflammatory profile throughout the course of Z infection in animals at P3 and P7. Among the cytokines analyzed, *Il6* expression showed a marked temporal increase, rising approximately 3.9-fold from P3 to P7, whereas *Tnf* and *Il1b* levels remained relatively stable over this interval despite remaining elevated compared with mock controls. A similar temporal amplification was observed for ISGs, with *Ifit1* and *Oas1g* increasing approximately 2.2-fold and 2-fold, respectively, from P3 to P7. In contrast, the expression of the interferon receptor subunits *Ifnar1* and *Ifnar2* remained

unchanged over time, suggesting that the evolving antiviral response during infection progression is primarily driven by downstream interferon signaling rather than changes in receptor expression.

Notably, the P3-P7 interval corresponds to a critical period of postnatal brain maturation, during which the hippocampal dentate gyrus undergoes active structural organization[42]. Postnatal ZIKV infection has been shown to disrupt dentate gyrus architecture, reduce neuronal populations, and promote astrogliosis and microglial activation[25]. Because reactive glial cells and elevated pro-inflammatory cytokines can negatively impact neurogenesis and synaptic maturation[43], sustained inflammatory and IFN signaling during this vulnerable developmental window may influence molecular pathways beyond direct viral cytopathology.

Transcriptional modulation of IFNAR components has been described as part of feedback mechanisms controlling prolonged IFN-I signaling[44], and several viruses, including ZIKV, can interfere with IFNAR signaling as an immune evasion strategy[45–47]. As key effectors of the IFN response, the OAS family plays a vital role in restricting viral replication. Notably, the enzymatically active *Oas1g* isoform functions to potentiate the viral RNA-driven interferon pathway[48]. The pronounced upregulation of ISGs, including *Oas1g* and *Ifit1*, therefore indicates sustained activation of antiviral pathways involving IFN response during infection progression.

In this context, the decreases in POP activity observed at P7 may represent a downstream consequence of prolonged IFN-I signaling in neonatal brain. This interpretation is supported by the observation that exogenous IFN-β administration recapitulated the virus-induced reduction in POP activity. Because viral infection and IFN-β exposure are both known to promote IFNAR1 downregulation[45], the present findings suggest a potential convergence between viral immune evasion mechanisms and host regulatory pathways controlling sustained IFN signaling.

Although POP inhibition has been proposed to be beneficial in certain inflammatory and degenerative conditions[36,37], its role during viral neuroinfection has not previously been explored. Under typical neuroinflammatory conditions, POP acts as a pro-inflammatory mediator, facilitating immune cell infiltration and macrophage activation[22]. However, our findings reveal a significant reduction in POP activity at later stages of infection, but not at early phases despite the demonstrated significant acute inflammatory responses. We propose that this modulation emerges from the interaction between antiviral IFN signaling and the developmental state of the brain. While early inflammatory responses did not alter POP activity, the reduction observed at P7 coincides with a developmental stage characterized by increased neuronal maturation and circuit formation. In this context, IFN-I signaling may contribute to the regulation of POP activity during infection, indicating that the observed enzymatic modulation reflects the convergence of antiviral immune responses and developmental processes in the neonatal brain. Consequently, the delayed reduction in POP activity appears to be a secondary consequence of the brain's persistence and potentially saturated IFN signaling. This is in line with the demonstrated decreases in POP activity in response to immunotherapy with IFN-alpha[38,49].

Notably, the temporal modulation of POP activity observed in our model coincided with alterations in neurotrophic signaling. In our hands, *Bdnf* expression displayed a dynamic profile in response to ZIKV infection, with reduced levels at early stages of infection followed by a significant increase at P7. This pattern suggests that neurotrophic pathways may become engaged during later stages of infection, potentially reflecting adaptive responses aimed at preserving neuronal integrity in the context of sustained neuroinflammatory signaling. Previous work has shown that reduction in POP expression occurs alongside changes in neurotrophic factors expression under conditions that disrupt neuronal plasticity and cognitive function[50]. Given the critical role of BDNF in neuronal survival, synaptic maturation, and neurogenesis[30,31], dysregulation of neurotrophic signaling during ZIKV infection may intersect with mechanisms implicated in virus-associated neurodevelopmental abnormalities.

To our knowledge, this study provides the first evidence that POP activity is modulated during viral infection of the developing brain. While previous studies have associated POP with inflammatory and neurodegenerative conditions, our findings indicate that POP activity is not directly influenced by the early cytokine-driven inflammatory response induced by ZIKV infection.

Together, the present findings suggest that POP modulation during ZIKV infection may emerge from the interaction between antiviral IFN signaling and the developmental state of the brain. Given the established roles of POP in neuroactive peptide processing and neuronal plasticity[31], the suppression of its activity during critical neurodevelopmental window may represent an adaptive response to antiviral signaling. However, this prolonged suppression could inadvertently disrupt pathways essential for neurodevelopmental homeostasis.

Although our findings demonstrate that activation of IFN-I signaling is sufficient to recapitulate the virus-induced reduction of POP activity, the precise molecular mechanisms underlying this regulation remain unknown. Future studies are planned to determine whether IFN signaling modulates POP through transcriptional regulation, post-translational mechanisms, or indirect effects mediated by the antiviral immune environment.

4. Material and Methods

4.1 Animals

The animals employed in this study were newborn Swiss mice (day 0, of either sex) from an institutional facility (CCS - UFRJ). A total of 112 neonatal animals were used and divided into two independent experimental cohorts. The first cohort consisted of 61 animals, while the second consisted of 51, from which 6 animals were excluded from the experiments due to fatal cases before the scheduled brain tissue sample collection. The data were initially analysed by cohort to verify reproducibility, and they were subsequently grouped after statistical homogeneity between cohorts was confirmed. Swiss mice were housed in the Animal Care Facility of the Microbiology Institute of the Federal University of Rio de Janeiro (UFRJ) and maintained in standard animal housing in 21 × 32 × 20 cm cages (4 mice per cage)

with food and water *ad libitum*, and light/dark cycles of 12 h each. The animals were euthanized by decapitation, after anaesthesia with ketamine (120 mg/kg) and xylazine (12 mg/kg). Groups were treated and assessed in an arbitrary order. Experiments and treatments were preferentially performed in the morning. Animals' general well-being was assessed by using a numerical score to classify the condition of the animal through the following parameters: body weight, general appearance, posture, behaviour/activity and breathing pattern. Animals were maintained in accordance with the guidelines of the Committee on Care and Use of Laboratory Animal Resources from National Research Council (USA). The Ethical Committee of the Universidade Federal do Rio de Janeiro (UFRJ) approved this study under protocol #A06/22-153-19, and the Universidade Federal de São Paulo (EPM/UNIFESP) approved this study under CEUA No 3322141024. No randomization or blinding methods were used for the animals, although the samples identifications were blind for the experimenters who determined and analysed the enzyme activity and the immune markers.

4.2 ZIKV propagation and titration

A Brazilian strain of Zika virus ($ZIKV^{BR}$; Recife/Brazil, ZIKV PE/243, number KX197192.1), and an African ZIKV strain ($ZIKV^{AF}$; MR766 - Uganda/Africa, number NC012532.1) was used in the experimental procedures. The viral propagation was conducted in C6/36 cellular cultures. The cells were inoculated with ZIKV at a multiplicity of infection (MOI) of 0.1 and subsequently incubated at a temperature of 28°C for one hour. Following this incubation, the inoculum was discarded and substituted with growth media enriched with 2% foetal bovine serum (FBS), and the cultures were maintained for additional five days. The conditioned medium was collected, subjected to centrifugation at 300 ·g, and sterile filtered to eliminate both cellular components and debris. Viral stocks were preserved at a temperature of − 80°C. ZIKV titres were assessed through plaque assays conducted on Vero cells, following established methodologies[4,51] and as previously applied by our group under identical experimental conditions.[29,52] As a negative control, the conditioned medium from uninfected C6/36 cells (prepared identically to the viral propagation procedure) was employed to mock-infect the animals.

4.3 ZIKV infection and treatment with IFNβ

On postnatal day 0 (P0), mice were anaesthetized by hypothermia and infected via the intracerebroventricular (ICV) route with 30 plaque-forming unit (PFU) of $ZIKV^{BR}$, $ZIKV^{AF}$ or uninfected C6/36 conditioned medium (mock) in a volume of 1.5 µL. The brains were collected at P3 or P7, immediately frozen, and stored at -80°C until use. In addition, P0 mice were alternatively infected by IP route injection of 100 PFU of $ZIKV^{BR}$ or of uninfected C6/36 conditioned medium (mock), which brains were collected at P7.

Treatment with interferon beta (IFNβ) was also performed after infection of mice at P0 mice with 30 PFU of $ZIKV^{BR}$ via the ICV route, following the treatment with 10 µg/mL IFNβ (R&D Systems, Catalogue Number 8234-MB) in 1 µL, injected into the lateral ventricle on days 2-, 4-, and 6-days post-infection (dpi). The ZIKV load in brain tissue was confirmed by RT-qPCR, as previously described.[29]

4.4 Preparation of brain homogenates

The soluble fraction of brain homogenates of 96 mice were individually prepared, briefly the brain samples were homogenized in 50 mM Tris-HCl pH 7.5 with 500 mM NaCl buffer (4 mL/g of tissue weight), in a cold wet-ice bath, using a Polytron homogenizer (Fisher Scientific, Hampton, VA, USA). This homogenization process consisted of three cycles, lasting for 30 s each, with a 1 min interval between each cycle. Then, samples were centrifuged at 20,000 ×g, for 10 min, at 4°C. The resulting precipitate was resuspended in the same buffer, and centrifuged once more at 20,000 ×g, for 90 min, at 4°C. The supernatant was discarded, and the precipitate was resuspended in the same buffer, now containing 0.5% Triton X-100. This mixture was allowed to stand for 1 h on ice bath before a new centrifugation at 5,000 ×g, for 10 min, at 4°C. The supernatant was used to measure POP activity and the protein concentration of these samples by employing the Bradford Protein Assay reagent (Bio Rad, Hercules, CA, USA).

4.5 Reverse Transcription and Quantitative Real-Time PCR (RT-qPCR)

Total RNA was extracted from mouse brain tissue using TRIzol™ Reagent (Thermo Fisher Scientific, Waltham, MA, USA; Cat. No. 15596026), following the manufacturer's protocol. Tissue homogenization was performed using a Polytron® homogenizer to ensure efficient cell disruption and RNA release. RNA concentration and purity were assessed using a NanoDrop 2000c spectrophotometer (Thermo Fisher Scientific), and only samples with $A_{260/280}$ and $A_{260/230}$ ratios above 1.8 were used for further analysis, indicating minimal protein and phenol contamination.

Complementary DNA (cDNA) was synthesized from 100 ng of total RNA using the SuperScript™ IV First-Strand Synthesis System (Invitrogen, Cat. No. 4368814), following the manufacturer's protocol. Quantitative PCR was performed using Power SYBR™ Green PCR Master Mix (Applied Biosystems, Cat. No. 18091200) on a 7500 Real-Time PCR System (Applied Biosystems). Gene-specific validated primers (Sequence 5' → 3') were purchased from Exxtend (São Paulo, Brazil) for the following mouse (Ms) targets:

Gene	Forward	Reverse
Tnf	CCCTCACACTCAGATCATCTTCT	GCTACGACGTGGGCTACAG
Il6	TTCTTGGGACTGATGCTGGTG	CAGAATTGCCATTGCACAACTC
Il1b	GTAATGAAAGACGGCACACC	ATTAGAAACAGTCCAGCCCA
Ifnar1	CTGGTCTGTGAGCTGTACTT	TCCCCGCAGTATTGATGAGT
Ifnar2	CTATCGTAATGCTGAAACGG	GTAATTCCACAGTCTCTTCT
Oas1g	CAGAAAAGCCAGGCCTGTG	CTCCTCCACCTGCTCAAAAG
Ifit1	ACTGAGGCCCACATTTGAGA	GGGTGATTGCCTTGTCTTCTG
Bdnf	GGCTGACACTTTTGAGCACGTC	CTCCAAAGGCACTTGACTGCTG
Actb	CAACTTGATGTATGAAGGCTTTGGT	ACTTTTATTGGTCTCAAGTCAGTGTACA

All reactions were performed in technical triplicates and *Actb* was used as the endogenous control. Melting curve analysis was conducted at the end of each run to confirm amplification specificity. The fluorescence threshold (Ct) was manually set based on appropriate negative and positive controls and was applied uniformly across all samples and experimental conditions. Relative gene expression was calculated using the $^{\Delta}$Ct and $^{\Delta\Delta}$Ct methods, with expression levels normalized to *Actb* and expressed relative to the corresponding control group. Data was presented as fold change ± SD.

4.6 POP activity measurements

POP enzymatic activity was determined using the fluorogenic FRET substrate Z-Gly-Pro-AMC (Bachem, NC 1103032). Reactions were performed in black 96-well plates in phosphate-buffered saline (PBS) pH 7.4 containing 1 mM dithiothreitol (DTT), with 10–20 µg of total protein in a final volume of 200 µL. The fluorescence increase due to the release of 7-amino-4-methylcoumarin (AMC) was measured using a Varioskan LUX Multimode Microplate Reader (Thermo Fisher Scientific) at λ_{Ex} = 380 nm; λ_{Em} = 460 nm, at 37°C for 30 min, with readings every 60 s. The amount of AMC released was calculated from a standard curve generated with free AMC (0–10 µM). Samples were analyzed in triplicate. POP specificity was confirmed by pre-incubating the samples with the selective inhibitor Z-Pro-prolinal (ZPP, 10 µM) for 15 min prior to POP specific substrate addition, as previously described.[53] POP activity was expressed as µM/min.mg^{-1} of protein. Protein concentration was determined by Bradford method.

4.7 Data and statistical analysis

All statistical analyses were performed using GraphPad Prism software (version 9.5.1). Each data point represents one brain hemisphere obtained from individual mice. Statistical evaluation was performed using ordinary t test, one-way ANOVA or two-way ANOVA, as described in the corresponding figure legends. When significant main effects or interactions were detected, multiple comparisons post hoc tests were performed to determine differences between individual groups. Homogeneity of variances

was evaluated using Brown–Forsythe and Bartlett's tests, as described in the corresponding figure legends. The significance level was set at 0.05 ($p \leq 0.05$). Data are presented as mean ± SEM or as box-and-whisker plots with individual data points. Statistical significance was defined as follows: ns, not significant; *$p \leq 0.05$; **$p \leq 0.01$; ***$p \leq 0.001$; ****$p \leq 0.0001$.

Declarations

Data Availability Statement

All data in this study are included in this published article and its additional files.

Ethics Statement

All experimental procedures involving mice were carried out in accordance with the Brazilian National Law (11.794/2008), the Guide for the Care and Use of Laboratory Animals of the Brazilian National Council of Animal Experimentation (CONCEA), and the ARRIVE guidelines. The Ethical Committee of the Universidade Federal do Rio de Janeiro (UFRJ) approved this study under protocol #A06/22-153-19, and the Universidade Federal de São Paulo (EPM/UNIFESP) approved this study under CEUA No 3322141024.

Credit Authorship Contribution Statement

APX: Conceptualization, investigation, methodology, formal analysis, validation, visualization, writing - original draft, review & editing. **ISF:** Conceptualization, investigation, methodology, formal analysis, validation, visualization, writing - original draft, review & editing. **WYO:** Investigation, methodology, formal analysis, validation. **LB:** Investigation, methodology. **RRC:** Investigation, methodology, validation, writing - review & editing. **LMH:** Investigation, methodology, validation, writing - review & editing. **PPG:** Methodology, resources, validation, writing - review & editing. **MAFH:** Conceptualization, methodology, resources, writing - original draft, review & editing, validation, supervision, project administration, funding acquisition.

Funding

This work was supported by FAPESP (Fundação de Amparo à Pesquisa do Estado de São Paulo) [No. 2022/00527-8; 2020/01107-7; 2019/13112-8; (INCT 2014 - TRANSLATIONAL MEDICINE)], FINEP (04.16.0054.02), CAPES and CNPq [INCT 408474/2024-6]. MAF Hayashi is also a recipient of a fellowship from CNPq [39337/2016-0 and 310057/2023-0]. These co-authors are recipient of a Fellowship from FAPESP: Ingrid S. de Farias [No. 2025/01121 3]; Leonardo Basso [No. 2024/04617-7]; William Y. Oyadomari [No. 2023/07904-4].

Conflicts of Interest

The authors declare that they have no conflicts of interest.

References

1. Pawitwar, S. S. et al. Overview on the Current Status of Zika Virus Pathogenesis and Animal Related Research. *J. Neuroimmune Pharmacol.* **12**, 371–388 (2017).
2. Peng, J. et al. Biased virus transmission following sequential coinfection of Aedes aegypti with dengue and Zika viruses. *PLoS Negl. Trop. Dis.* **18**, e0012053 (2024).
3. De Vilharba, A. Disease burden of congenital Zika virus syndrome in Brazil and its association with socioeconomic data. *Sci. Rep.* **13**, 11882 (2023).
4. Garcez, P. P. et al. Zika virus impairs growth in human neurospheres and brain organoids. *Science* **352**, 816–818 (2016).
5. Cugola, F. R. et al. The Brazilian Zika virus strain causes birth defects in experimental models. *Nature* **534**, 267–271 (2016).
6. Shao, Q. et al. The African Zika virus MR-766 is more virulent and causes more severe brain damage than current Asian lineage and Dengue virus. *Development* dev.156752 (2017). 10.1242/dev.156752
7. Brown, A. J. et al. Comparative susceptibility of Old World and New World bat cell lines to Zika virus: Insights into viral replication and inflammatory responses. *PLoS Negl. Trop. Dis.* **20**, e0014065 (2026).
8. Mlakar, J. et al. Zika Virus Associated with Microcephaly. *N Engl. J. Med.* **374**, 951–958 (2016).
9. Schneider, W. M., Chevillotte, M. D. & Rice, C. M. Interferon-Stimulated Genes: A Complex Web of Host Defenses. *Annu. Rev. Immunol.* **32**, 513–545 (2014).
10. Dalskov, L., Gad, H. H. & Hartmann, R. Viral recognition and the antiviral interferon response. *EMBO J.* **42**, e112907 (2023).
11. Savidis, G. et al. The IFITMs Inhibit Zika Virus Replication. *Cell. Rep.* **15**, 2323–2330 (2016).
12. Richardson, R. B. et al. A CRISPR screen identifies IFI6 as an ER-resident interferon effector that blocks flavivirus replication. *Nat. Microbiol.* **3**, 1214–1223 (2018).
13. Xia, H. et al. An evolutionary NS1 mutation enhances Zika virus evasion of host interferon induction. *Nat. Commun.* **9**, 414 (2018).
14. Grant, A. et al. Zika Virus Targets Human STAT2 to Inhibit Type I Interferon Signaling. *Cell. Host Microbe*. **19**, 882–890 (2016).
15. Krenn, V. et al. Organoid modeling of Zika and herpes simplex virus 1 infections reveals virus-specific responses leading to microcephaly. *Cell. Stem Cell.* **28**, 1362–1379e7 (2021).
16. Tenorio-Laranga, J. et al. The expression levels of prolyl oligopeptidase responds not only to neuroinflammation but also to systemic inflammation upon liver failure in rat models and cirrhotic patients. *J. Neuroinflammation*. **12**, 183 (2015).
17. Natunen, T. A., Gynther, M., Rostalski, H., Jaako, K. & Jalkanen, A. J. Extracellular prolyl oligopeptidase derived from activated microglia is a potential neuroprotection target. *Basic. Clin. Pharma Tox*. **124**, 40–49 (2019).

18. Kilpeläinen, T. et al. Novel PREP ligand, HUP-46, ameliorates behavioral deficits in an alpha-synuclein based Parkinson's disease model. *Exp. Neurol.* **397**, 115593 (2026).
19. Walter, R., Shlank, H., Glass, J. D., Schwartz, I. L. & Kerenyi, T. D. Leucylglycinamide Released from Oxytocin by Human Uterine Enzyme. *Science* **173**, 827–829 (1971).
20. Serfozo, P. et al. Ang II (Angiotensin II) Conversion to Angiotensin-(1–7) in the Circulation Is POP (Prolyloligopeptidase)-Dependent and ACE2 (Angiotensin-Converting Enzyme 2)-Independent. *Hypertension* **75**, 173–182 (2020).
21. Kumar, N. & Yin, C. The anti-inflammatory peptide Ac-SDKP: Synthesis, role in ACE inhibition, and its therapeutic potential in hypertension and cardiovascular diseases. *Pharmacol. Res.* **134**, 268–279 (2018).
22. Tenorio-Laranga, J., Coret-Ferrer, F., Casanova-Estruch, B., Burgal, M. & García-Horsman, J. A. Prolyl oligopeptidase is inhibited in relapsing-remitting multiple sclerosis. *J. Neuroinflammation*. **7**, 23 (2010).
23. Breen, G. et al. Two peptidase activities decrease in treated bipolar disorder not schizophrenic patients. *Bipolar Disord.* **6**, 156–161 (2004).
24. Casili, G. et al. The Protective Role of Prolyl Oligopeptidase (POP) Inhibition in Kidney Injury Induced by Renal Ischemia–Reperfusion. *IJMS* **22**, 11886 (2021).
25. Xu, P., Yu, Y. & Wu, P. Role of microglia in brain development after viral infection. *Front. Cell. Dev. Biol.* **12**, 1340308 (2024).
26. Kölliker-Frers, R. et al. Neuroinflammation: An Integrating Overview of Reactive-Neuroimmune Cell Interactions in Health and Disease. *Mediators of Inflammation.* 9999146 (2021). (2021).
27. Kowiański, P. et al. BDNF: A Key Factor with Multipotent Impact on Brain Signaling and Synaptic Plasticity. *Cell. Mol. Neurobiol.* **38**, 579–593 (2018).
28. Miranda, M., Morici, J. F., Zanoni, M. B. & Bekinschtein, P. Brain-Derived Neurotrophic Factor: A Key Molecule for Memory in the Healthy and the Pathological Brain. *Front. Cell. Neurosci.* **13**, 363 (2019).
29. Christoff, R. R. et al. Assessing the role of Ndel1 oligopeptidase activity in congenital Zika syndrome: Potential predictor of congenital syndrome endophenotype and treatment response. *J. Neurochem.* **166**, 763–776 (2023).
30. Di Daniel, E. et al. Prolyl oligopeptidase binds to GAP-43 and functions without its peptidase activity. *Mol. Cell. Neurosci.* **41**, 373–382 (2009).
31. Höfling, C. et al. Deficiency of prolyl oligopeptidase in mice disturbs synaptic plasticity and reduces anxiety-like behaviour, body weight, and brain volume. *Eur. Neuropsychopharmacol.* **26**, 1048–1061 (2016).
32. Chen, X. Z. et al. Study on the spatiotemporal regulation of interferon-stimulated genes during Zika virus infection. *Front. Immunol.* **16**, 1702266 (2026).
33. Tiwari, S. K. et al. Zika virus infection reprograms global transcription of host cells to allow sustained infection. *Emerg. Microbes Infections*. **6**, 1–10 (2017).

34. Benazzato, C. et al. Zika virus vertical transmission induces neuroinflammation and synapse impairment in brain cells derived from children born with Congenital Zika Syndrome. *Sci. Rep.* **14**, 18002 (2024).
35. Ganguli, S. & Chavali, P. L. Intrauterine Viral Infections: Impact of Inflammation on Fetal Neurodevelopment. *Front. Neurosci.* **15**, 771557 (2021).
36. Payne, G. A. et al. Prolyl endopeptidase contributes to early neutrophilic inflammation in acute myocardial transplant rejection. *JCI Insight*. **6**, e139687 (2021).
37. Zhang, J. et al. Prolyl endopeptidase disruption reduces hepatic inflammation and oxidative stress in methionine-choline-deficient diet-induced steatohepatitis. *Life Sci.* **270**, 119131 (2021).
38. Van Gool, A. R. et al. Serum Activity of Prolyl Endopeptidase, but Not of Dipeptidyl Peptidase IV, Is Decreased by Immunotherapy with IFN- α in High-Risk Melanoma Patients. *J. Interferon Cytokine Res.* **24**, 411–415 (2004).
39. Hayashida, E. et al. Zika virus encephalitis in immunocompetent mice is dominated by innate immune cells and does not require T or B cells. *J. Neuroinflammation*. **16**, 177 (2019).
40. Shen, T. J., Chen, C. L., Jhan, M. K., Tseng, P. C. & Lin, C. F. CNS Immune Profiling in a Dengue Virus-Infected Immunocompetent Outbred ICR Mice Strain. *Front. Cell. Infect. Microbiol.* **10**, 557610 (2020).
41. Clancy, B., Darlington, R. B. & Finlay, B. L. Translating developmental time across mammalian species. *Neuroscience* **105**, 7–17 (2001).
42. Dang, J. et al. Zika Virus Depletes Neural Progenitors in Human Cerebral Organoids through Activation of the Innate Immune Receptor TLR3. *Cell. Stem Cell.* **19**, 258–265 (2016).
43. Wang, K. et al. Zika virus replication on endothelial cells and invasion into the central nervous system by inhibiting interferon β translation. *Virology* **582**, 23–34 (2023).
44. Ivashkiv, L. B. & Donlin, L. T. Regulation of type I interferon responses. *Nat. Rev. Immunol.* **14**, 36–49 (2014).
45. Kumar, A. et al. Zika virus inhibits type-I interferon production and downstream signaling. *EMBO Rep.* **17**, 1766–1775 (2016).
46. Yockey, L. J. et al. Type I interferons instigate fetal demise after Zika virus infection. *Sci. Immunol.* **3**, eaao1680 (2018).
47. Shemesh, M., Lochte, S., Piehler, J. & Schreiber, G. IFNAR1 and IFNAR2 play distinct roles in initiating type I interferon–induced JAK-STAT signaling and activating STATs. *Sci. Signal.* **14**, eabe4627 (2021).
48. Elkhateeb, E. et al. The role of mouse 2',5'-oligoadenylate synthetase 1 paralogs. *Infect. Genet. Evol.* **45**, 393–401 (2016).
49. Van Gool, A. R. et al. Plasma Activity of Prolyl Endopeptidase in Relation to Psychopathology During Immunotherapy with IFN- α in Patients with Renal Cell Carcinoma. *J. Interferon Cytokine Res.* **28**, 283–286 (2008).

50. Shirenova, S. D., Khlebnikova, N. N. & Krupina, N. A. Long-Term Social Isolation Reduces Expression of the BDNF Precursor and Prolyl Endopeptidase in the Rat Brain. *Biochem. Mosc.* **86**, 704–715 (2021).
51. Contreras, D. & Arumugaswami, V. Zika Virus Infectious Cell Culture System and the In Vitro Prophylactic Effect of Interferons. *JoVE* **54767** 10.3791/54767 (2016).
52. Oyadomari, W. Y. et al. Infection by zika virus increase angiotensin I-converting enzyme activity in mouse brain. *Biochimie* **227**, 116–118 (2024).
53. Marins, L. A. N. et al. Prolyl oligopeptidase activity (POP) in early stage and medicated schizophrenia and in an animal model for schizophrenia study: In vivo effects of psychopharmacological substances on enzyme activity. *Brain Disorders*. **10**, 100075 (2023).

Figures

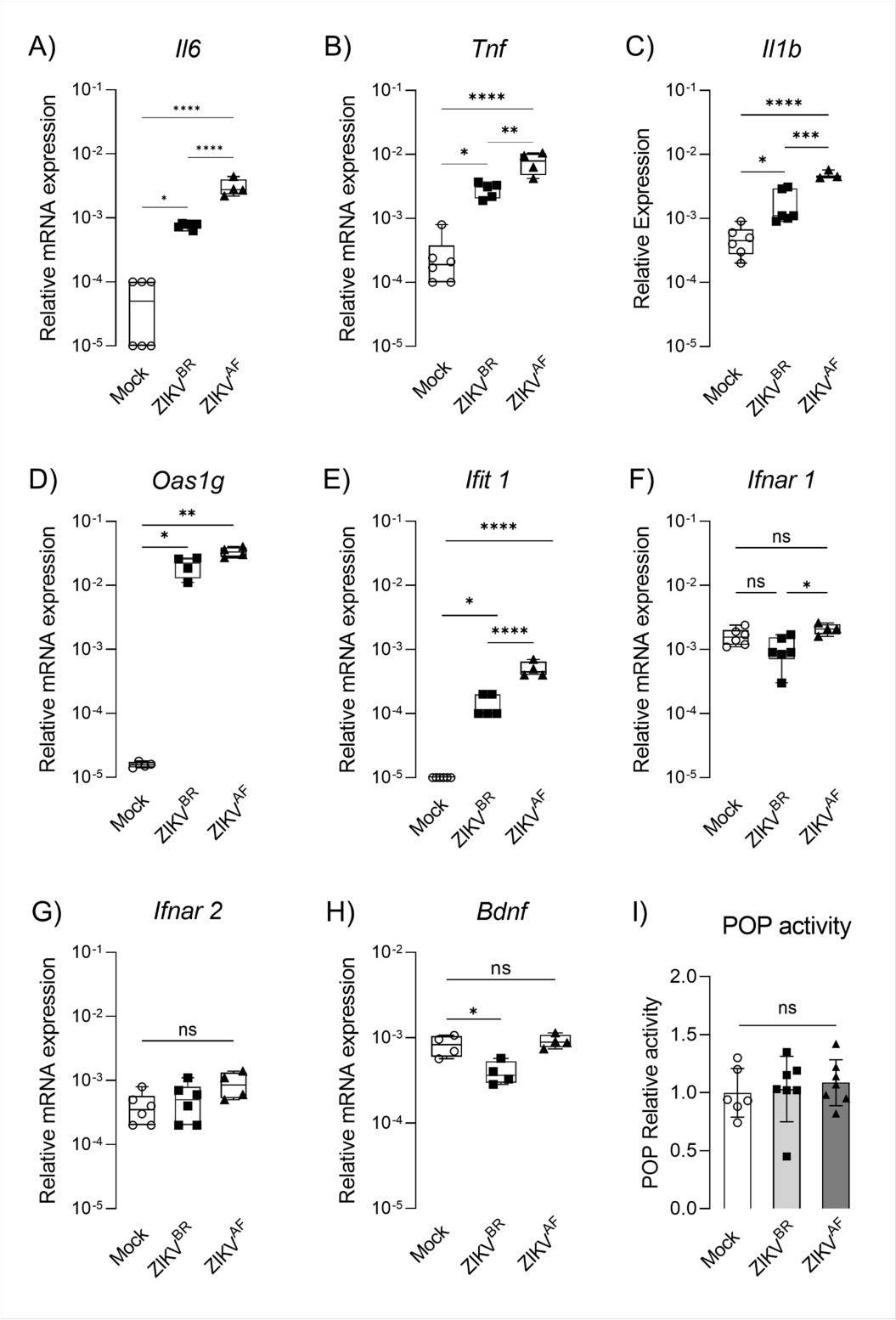


Figure 1

Differential modulation of innate immune gene expression by ZIKV strains without changes in POP activity at P3. Neonatal mice were infected by intracerebroventricular (ICV) injection with the Brazilian ($ZIKV^{BR}$) or African ($ZIKV^{AF}$) ZIKV strain, and brain tissue was collected at postnatal day 3 (P3). (**A-H**) Relative mRNA expression of the indicated genes, calculated using the $2^{-\Delta Ct}$ method and normalized to *Actb*. (**I**) Prolyl oligopeptidase (POP) activity measured in brain homogenates. For gene expression

analyses, *n* = 6 for mock, *n* = 6 for ZIKV^{BR}, and *n* = 4 for ZIKV^{AF}. For POP activity, *n* = 6 for mock, *n* = 7 for ZIKV^{BR}, and *n* = 7 for ZIKV^{AF}. Data are presented as mean ± SD. Statistical significance was determined using one-way ANOVA followed by Tukey's multiple comparisons test. ns, not significant; **p* < 0.05; ***p* < 0.01; ****p* < 0.001; *****p* < 0.0001.

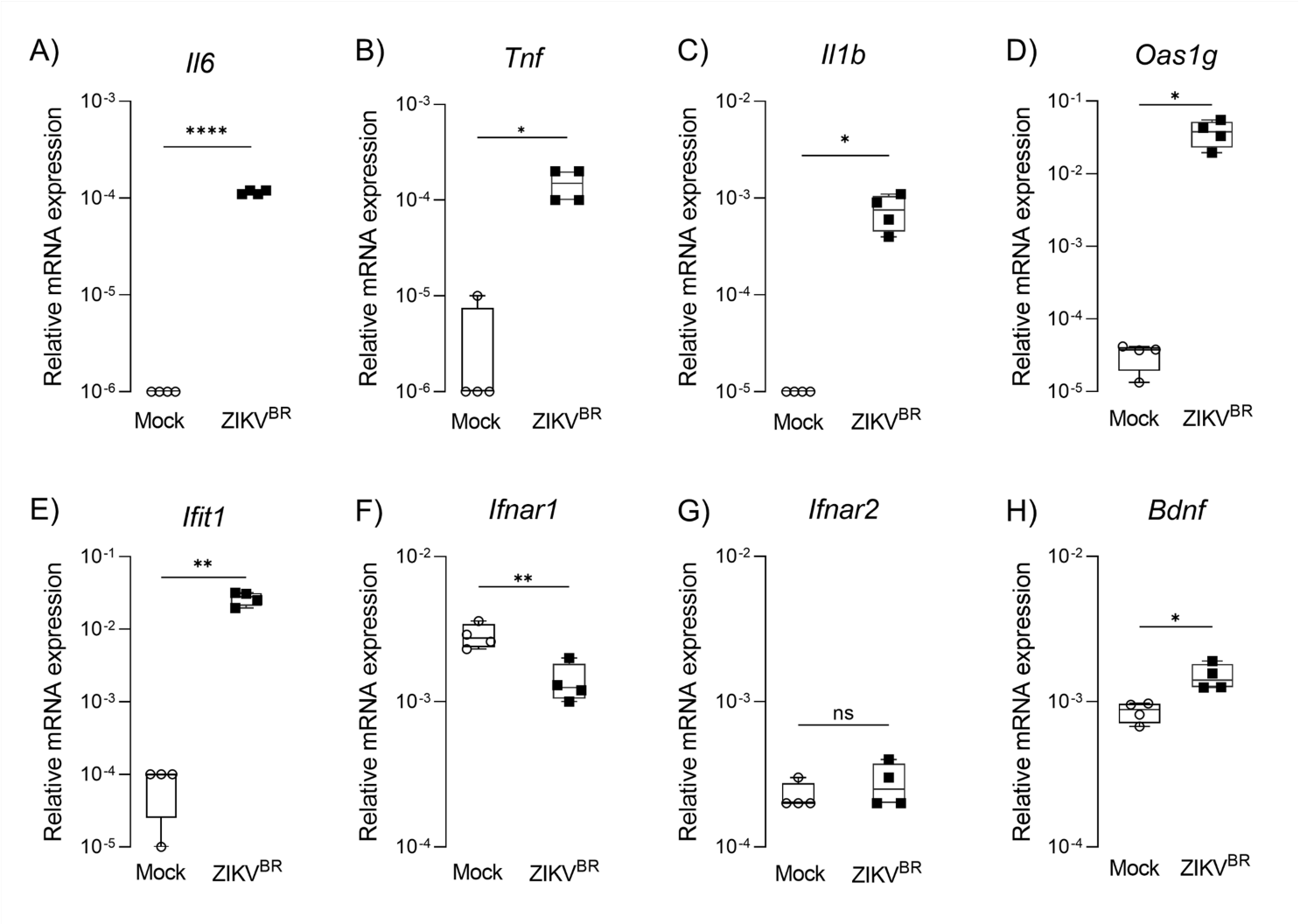


Figure 2

ZIKV^{BR} infection induces pro-inflammatory and interferon-related gene expression in neonatal mouse brains at P7. Neonatal mice were infected by intracerebroventricular (ICV) injection with the Brazilian ZIKV strain (ZIKV^{BR}), and brain tissue was collected at postnatal day 7 (P7). (**A-H**) Relative mRNA expression of the indicated genes calculated using the $2^{-\Delta Ct}$ method and normalized to *Actb*. For gene expression analyses, *n* = 4 for mock and *n* = 4 for ZIKV^{BR}. Data are presented as mean ± SD. Statistical significance was determined using unpaired t test with Welch's correction; ns, not significant; **p* < 0.05; ***p* < 0.01; *****p* < 0.0001.

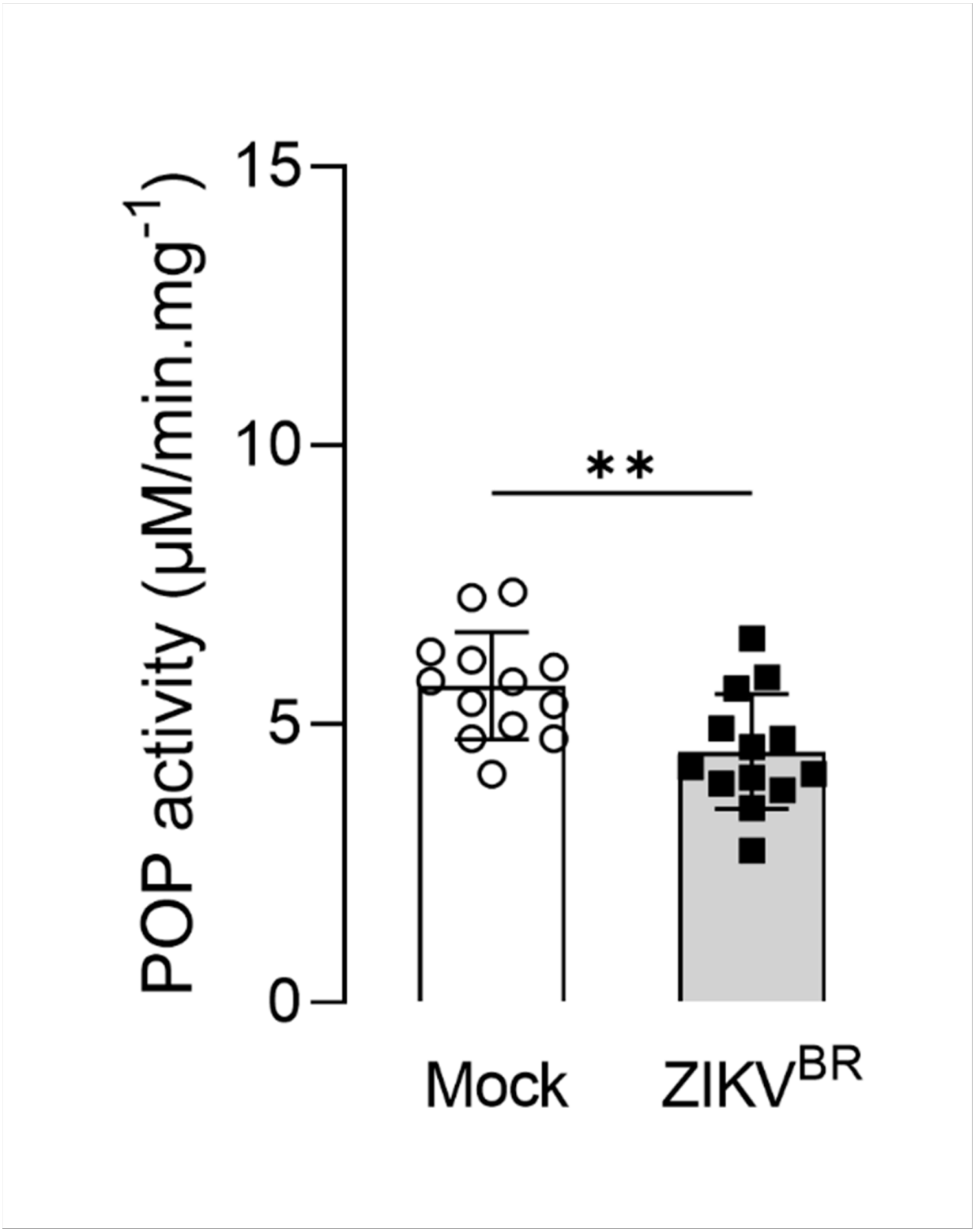


Figure 3

ZIKV^{BR} infection reduces POP activity in neonatal mouse brains at P7. Prolyl oligopeptidase (POP) activity was measured in brain homogenates from neonatal mice at postnatal day 7 (P7) following intracerebroventricular (ICV) infection with ZIKV^{BR} compared with mock controls. Each data point represents an individual animal. n = 13 for mock and n = 13 for ZIKV^{BR}. Data are presented as mean ± SD. Statistical significance was determined using unpaired t test with Welch's correction; **p < 0.01.

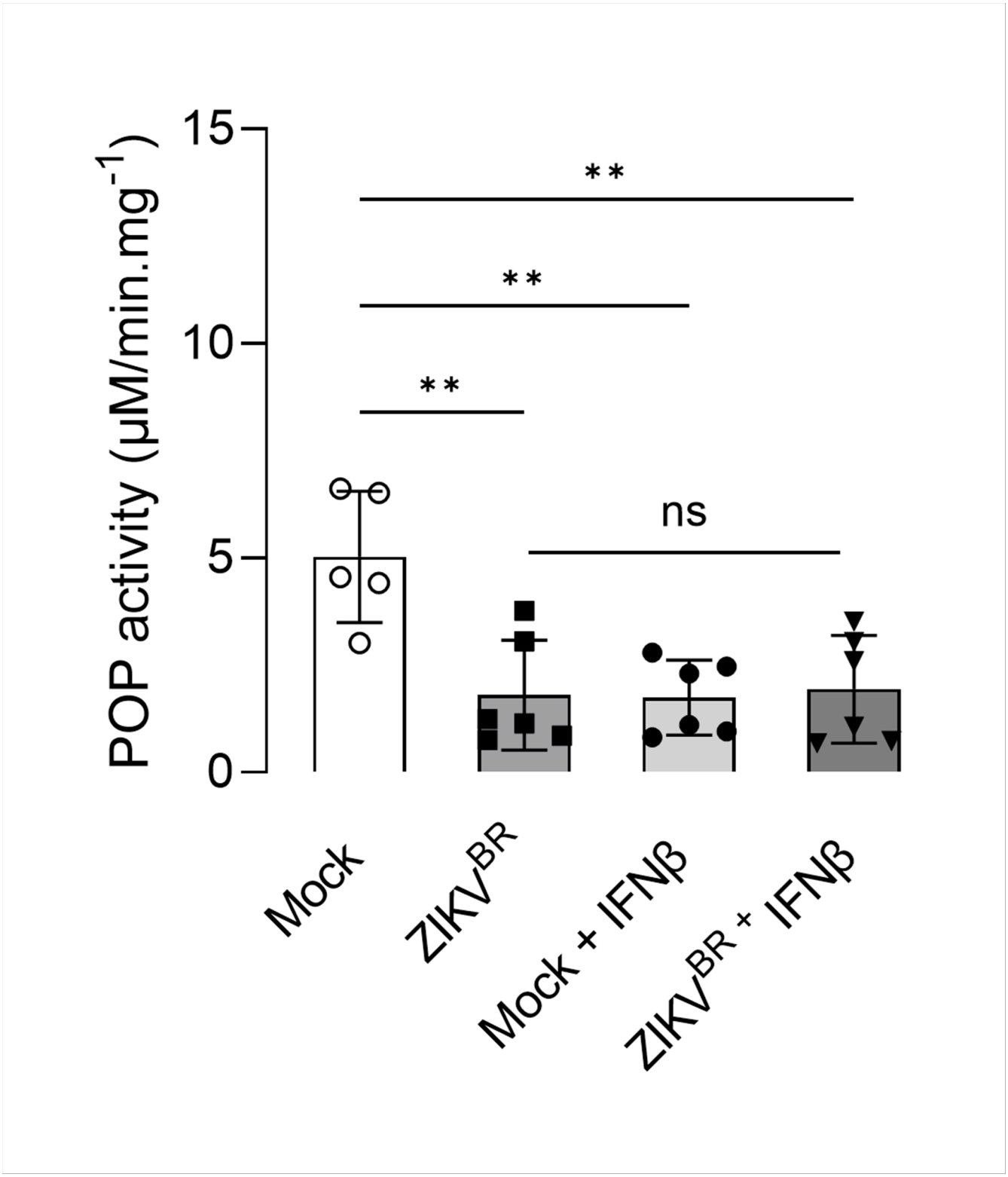


Figure 4

Exogenous IFN-β mimics the effect of ZIKVBR infection on POP activity in neonatal mouse brains. Neonatal mice were treated with exogenous IFN-β prior to intracerebroventricular (ICV) infection with $ZIKV^{BR}$, and prolyl oligopeptidase (POP) activity was measured in brain homogenates at postnatal day 7 (P7). Data are expressed as relative activity normalized to the mock group (100%). Each data point represents an individual animal. *n* = 5 for mock, *n* = 6 for $ZIKV^{BR}$, *n* = 6 for mock + IFN-β, and *n* = 6 for

$ZIKV^{BR}$ + IFN-β. Data are presented as mean ± SD. Statistical significance was determined using one-way ANOVA followed by Tukey's multiple comparisons test. ns, not significant; $P < 0.01$.

Supplementary Files

This is a list of supplementary files associated with this preprint. Click to download.

- SupplementalFig1.tif